

Person Verification Process Using Iris Information

Mireya S. García-Vázquez¹, Alejandro A. Ramírez-Acosta¹

¹ Instituto Politécnico Nacional-CITEDI, Av. Del Parque No.1310, Tijuana BC,
mgarciav@citedi.mx, alvaro@citedi.mx

Abstract. Biometric verification systems employing images of the iris are claimed to be extremely accurate. The iris biometrics features can be used on security systems applications, due to their great advantages, such as variability, stability and security. The speed and performance of an iris verification system is crucial. Thus in this paper, efficient verification process for iris recognition with important performance in feature extraction stage and high confidence is described. The proposed system uses 1D Log-Gabor filter for texture analysis. Experimental tests were performed using CASIA iris database.

Keywords: Iris, Recognition, biometrics.

1 Introduction

Iris recognition is one of important biometric recognition approach in a human identification. Using only iris pattern information, it has a higher accuracy rate than other biometric recognition methods such as face recognition, fingerprint recognition, voice recognition, and hand geometry, noting that an iris has much pattern information and is invariable through a lifetime [1-4]. Thus, iris recognition is in the limelight of security applications. There are mainly two iris recognition prototypes that had been developed: one by J. Daugman [1-2], and the other by W. Wildes [3]. Most of the commercial iris recognition systems are based on these prototypes [4-7]. However, one of the most successful commercial iris recognition systems is distributed by L1 identity solutions (known before as Iridian Technologies) [5] and it uses algorithms patented by Daugman. Eye images are captured by the system (Image Acquisition). Then, they are processed by first detecting and segmenting the iris (Preprocessing). The iris region of the image is warped (unrolled) to normalized rectangle. Features that represent the iris patterns are extracted and a code (template) is generated (Encode Features). And finally, verification is then achieved by matching the template against a gallery of templates using normalized Hamming distance (Matching codes).

The objective of this article is to describe an efficient verification process for iris recognition with important performance in feature extraction stage and high confidence. In this article the different concepts for every stage in an iris recognition system were

developed in C language in order to verify the system performance and to validate the chosen options for every stage. The Section 2 describes and analyzes each stage of the system that has been implemented. The experiments and results will be presented in the section 3. Finally conclusions will be drawn in section 4.

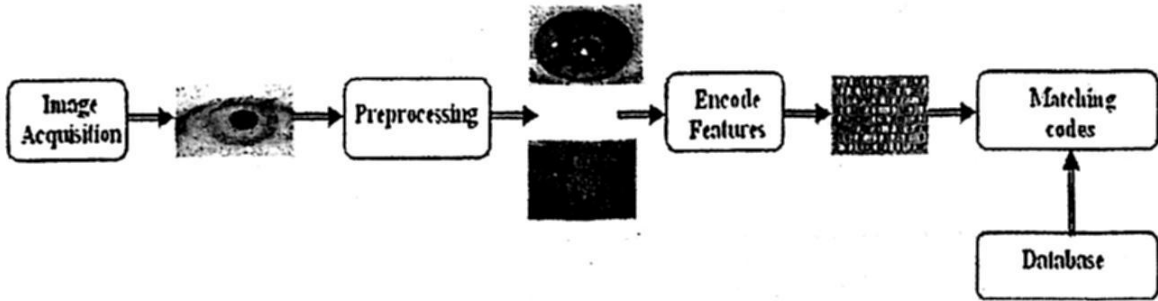


Fig. 1. How iris verification process work.

2 Iris Verification Process

2.1 Image Acquisition

One of the major challenges of automated iris verification system is to capture a high quality image of the iris while remaining noninvasive to the human operator. Given that the iris is a relatively small (1cm in diameter), dark object and that the people are very sensitive about their eyes, this matter required careful engineering. The following points should be concern: Desirable to acquire images of the iris with sufficient resolution and sharpness to support verification. It is important to have good contrast in the interior iris pattern without resorting to a level of illumination that annoys the subject. The images should be well framed (i.e. centered). Noises in the acquired images should be eliminated as much as possible.

2.2 Iris Localization

An eye image contains not only the iris region but also some unuseful parts, such as the pupil, eyelids, sclera, and so on. For this reason, at first step, segmentation will be done to localize and extract the iris region from the eye image. Iris localization is the detection of the iris area between pupil and sclera (see Fig. 2.a). So we need to detect the upper and lower boundaries of the iris and determine its inner and outer circles. The captured image is a 2-D array ($M \times N$) and is described as $I(x, y)$ where the point (x, y) is the gray-level. The first eye part to isolate is the pupil (dark circular area in an eye image, see Fig 2.b). It is used to fix a region threshold to binarize the image $I(x, y)$ to obtain an image $I_B(x, y)$. The image is scanned in the horizontal direction to find the longest chord which will be the diameter of the pupil. The following equations are used to find the centre coordinates [8]:

$$\begin{aligned} x_p &= x + \frac{Dia(x,y)}{2} \\ y_p &= y \end{aligned} \quad (1)$$

Dia is the longest chord, and (x, y) is the start point of *Dia*.

The outer boundary of the iris is more difficult to detect because of the low contrast between the two sides of the boundary. Canny edge detection is performed to create an edge map to generate gradients information [9]. Circular Hough Transform which is employed by Wildes [10], is used to detect the iris-sclera boundary to obtain a new centre (x_s, y_s) and radius r . The linear Hough Transform [11] is used to detect and to isolate eyelids and eyelashes.

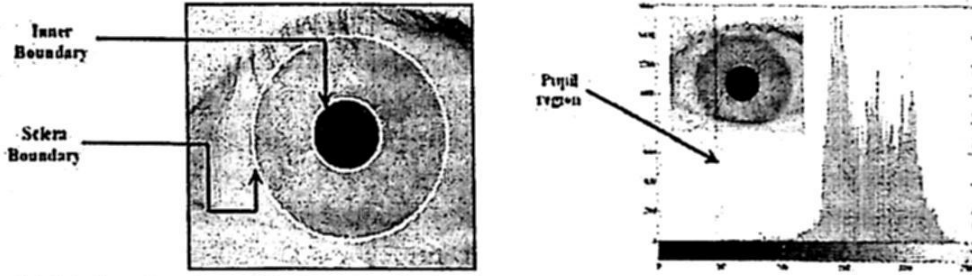


Fig. 2. (a) Iris localization. (b) Gray levels for the pupil region.

2.3 Iris Normalization

The irises captured from the different people have different sizes. The size of the irises from the same eye may change due to illumination variations, distance from the camera, or other factors. At the same time, the iris and the pupil are non concentric. These factors may affect the result of iris matching. In order to avoid these factors and achieve more accurate verification, the normalization for iris images is implemented. In normalizations, the iris circular region is transformed to a rectangular region with a fixed size. With the boundaries detected, the iris region is normalized from Cartesian coordinates to polar representation. This operation is done using the following operation:

$$I(x(r,\theta), y(r,\theta)) \rightarrow I(r,\theta) \quad (2)$$

with

$$x(r,\theta) = (1-r)x_p(\theta) + rx_s(\theta) \quad \text{and} \quad y(r,\theta) = (1-r)y_p(\theta) + ry_s(\theta)$$

The r is on the interval $[0,1]$ and θ is an angle $[0,2\pi]$. The $I(x,y)$ is the region image, (x,y) are the original Cartesian coordinates, (r,θ) are the corresponding normalized polar coordinates. The x_p, y_p and x_s, y_s are the coordinates of the iris ring along the θ direction.

Besides to generate the normalized iris image (iris template) is necessary to generate another image called "noise mask". This mask indicates the regions of the normalized iris where the pattern of the iris is obstructed by the eyelids, eyelashes, etc. The noise mask has the same dimensions that the iris image, it is used in the comparison stage to avoid to compares the obstructed regions.

2.4 Feature encoding

The iris has a particularly interesting structure and provides abundant texture information. So, it is desirable to explore representation methods which can describe global and local information in an iris. In this stage the iris features are obtained convolving the normalized iris pattern with a 1D Log-Gabor filters. Gabor Filters based methods have been widely used as feature extractor in computer vision, especially for texture analysis [12]. Gabor filters can serve as excellent band-pass filter for one-dimensional signals. Daugman [1,15] used multi-scale Gabor wavelets to extract phase structure information of the iris texture. However, Field [14] has examined that there is a disadvantage of the Gabor Filter in which the even symmetric filter will have a DC component whenever the bandwidth is larger than one octave. To overcome this disadvantage, another type of filter is used known as Log-Gabor, which is Gaussian on a logarithmic scale, can be used to produce zero DC components for any bandwidth. The Log-Gabor filters are obtained by multiplying the radial and angular components together where each even and odd symmetric pair of Log-Gabor filters comprises a complex Log-Gabor filter at one scale. The frequency response of a Log-Gabor Filters is given as:

$$G(f) = e^{\left(\frac{-(\log(f/f_0))^2}{2(\log(\beta/f_0))^2} \right)} \quad (3)$$

Where f_0 represents the central frequency, and β bandwidth of the filters.

The 1D Log-Gabor Filter is chosen to be the feature extractor of iris for the implementation since 1D Log-Gabor Filters is an improved version of Gabor Filters. By applying 1D Log-Gabor Filters, 2D normalized pattern is divided into a number of 1D signals, and these 1D signals are convolved with 1D Gabor wavelet. The rows of the 2D normalized pattern are taken as the 1D signal; each row corresponds to a circular ring on the iris region. The angular direction is taken rather than the radial one, which corresponds to columns of the normalized pattern, since maximum independence occurs in the angular direction. To encode each row of the image (X vector), the discrete Fourier transform (DFT) is applied to get vector Y (eq.4). Then vector Y and a 1-D log-Gabor wavelet are multiplied to get the vector Z (eq.5). The 1D Log-Gabor function is defined (eq.3), only one filter is used, with $f_0 = 12$, and a bandwidth $\beta = 0.5$ [15]. Finally, using the inverse DFT on the vector Z to get the vector D (eq.6).

$$Y_k = \sum_{n=1}^N x_n e^{-j2\pi(k-1)(n-1)/N} \quad (4)$$

$$z_k = Y_k \times G_k \quad (5)$$

$$D_k = \frac{1}{N} \sum_{n=1}^N z_k e^{-j2\pi(k-1)(n-1)/N} \quad (6)$$

The output of the Gabor filter are complex numbers, where the phase angle at each output point is quantized to two bits depending on the quadrant where this each element in the complex plane. Thus for an image normalized with size (MxN) the resulting template is of size (Mx2N). The template size with radial resolution of 128 pixels and angular resolution of 256 pixels was chosen. These parameters generate an iris template that contains 32768 bits of information.

2.5 Matching codes

Matching is a process to determine whether two iris templates are from the same individual. To perform the matching process, we will attempt to measure the Hamming Distance (HD) [1] between two iris templates. The Hamming distance between any two equal length binary vectors is simply the number of bits positions in which they differ divided by the length of the vectors.

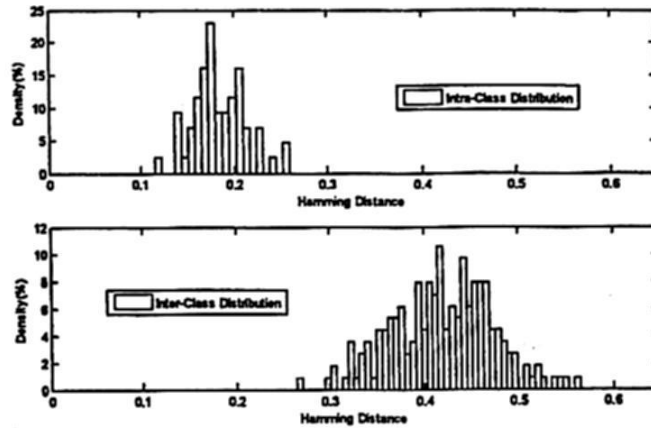


Fig. 3. Distributions of probability intra-class and inter-class in function to hamming distance.

Therefore, using the Hamming distance of two bit patterns, a decision can be made as to whether the two patterns were generated from different irises or from the same one. Since an individual iris region contains many features, each iris region will produce a bit-pattern which is independent to that produced by another iris, and two iris codes produced from the same iris will be highly correlated (intra-class comparisons). If two bits patterns are completely independent, such as iris templates generated from different irises (inter-class comparisons), the Hamming distance between the two patterns should equal 0.5. This occurs because independence implies the two bit patterns will be totally random, so there is 0.5 chance of setting any bit to 1, and vice versa. Therefore, half of the bits will agree and half will disagree between the two patterns. If two patterns are derived from the same

iris, the Hamming distance between them will be close to 0.0, since they are highly correlated and the bits should agree between the two iris codes. Although, in theory, two iris templates generated from the same iris will have a Hamming distance of 0.0, in practice this will not occur. Normalization is not perfect, and also there will be some noise that goes undetected, so some variation will be present when comparing two intra-class iris templates. The Hamming distance algorithm employed incorporates noise masking ($C(i, j)$), so that only significant bits are used in calculating the Hamming distance between two iris templates (A, B). Both iris mask (iris *maskA*, iris *maskB*) are used in the calculation. The Hamming distance will be calculated using only the bits generated from the true iris region given by the equation:

$$HD(A, B) = \frac{1}{\sum_{i,j} C(i, j)} \sum_{i,j} (A(i, j) \text{ xor } B(i, j) \& C(i, j))$$

where

$$C(i, j) = \begin{cases} 1 & \text{if } \text{maskA}(i, j) = 0 \text{ and } \text{maskB}(i, j) = 0; \\ 0 & \text{otherwise} \end{cases} \quad (7)$$

To make a recognition decision, a threshold X can be defined. If the obtained distance of Hamming is minor who thresholds X , is decided that the compared codes were generated by same eye, otherwise is decided that they were generated by different eyes. Both distributions Inter-class and intra-class, generally, are overlapped. For that reason, the area under the distribution Inter-class to the left of threshold X , represents the probability of a false identification, whereas the area under the distribution intra-class to the right of threshold X , represents the probability of a false rejection.

These measures are known as false acceptance rate (FAR) and false rejection rate (FRR), the FAR is the probability that an unauthorized subject is incorrectly accepted by the system whereas the FRR is the probability that an authorized subject is incorrectly rejected. The distance for both distributions ("decidability") can be calculate by equation (8), this value can be used to optimize the parameters on log-Gabor filters

$$d = \frac{|\mu_{INTRA} - \mu_{INTER}|}{\sqrt{\sigma_{INTRA}^2 + \sigma_{INTER}^2} / 2} \quad (8)$$

where

μ_{INTRA}, μ_{INTER} = the mean of the probability distributions

$\sigma_{INTRA}, \sigma_{INTER}$ = standard deviation of the probability distributions

3 Experiments

In order to evaluate the iris verification algorithms, CASIA (The Chinese Academy of Sciences Institute of Automation) iris image database is used [16]. This image database contains 756 eye images from 108 different persons. The experiments were performed in

C language on Pentium IV PC with 512 MB RAM and 1.8 GHz. The experiments were obtained with verifications, evaluating genuine matching scores for all the possible combinations (60 intra-class comparisons) and evaluating the impostor matching scores for all the possible combinations (190 inter-class comparisons). The parameters distributions obtained were $\mu_{INTRA} = .182$ $\sigma_{INTRA} = .029$ for Intra-class distribution and $\mu_{INTER} = .4195$ $\sigma_{INTER} = .0534$ for Inter-class distribution. The calculated distance between the intra-class and the inter-class distribution was $d=5.52732$, and the portion that overlaps between the intra-class and the inter-class was very small (see fig. 3). This proves that the proposed features are highly discriminating. Acceptance Rate (FAR) and False Rejection Rate (FRR) are the two critical measurements of system effectiveness. The values of FAR and FRR were 0.182516% and 0.185026% respectively. The EER (Equal Error Rate) was 0.202 %.The iris features (320 entries) were extracted with a bandwidth of $\beta=0.5$ with center wavelength $f_0=14$ pixels.

The method described in this implementation locates the iris in the image based on edge detection approach, whereas Daugman [1] makes use of a deformable model. In addition, several tests were made to obtain the time of execution for each stage in the implemented system. The average total execution time of a basic verification process not exceeds 500 ms, which is suitable for a recognition system.

The table 1 shows the comparative results of the time computation consumed by each block of the iris verification algorithms of four methods. As we can see, the experimental results have shown that the computational cost for Extraction features stage of our method consumes less time than the other methods (12.6ms). The Log-Gabor filter produces an uncorrelated and less redundant representation for iris texture compared with the ordinary Gabor Filters. Now, we are working on more precisely in Iris localization optimization (362.8 ms). Thus, we expect to further improve the performance of the current method.

Table 1. Time consuming for each stage of the different implemented systems

Operation	Daugman [2]	Tisee et all [17]	Avila et all [12]	Wildes [10]	Proposed
Iris localization	90 ms	250 ms	—	10 seg	362.8ms
Extraction features	102 ms	188 ms	229.5 ms		12.6 ms

4 Conclusions and Perspectives

The work presented in this paper involves the implementation of all phases of an iris recognition system. In order to verify the system performance and to validate the chosen options for every stage, the iris recognition system was developed in C language. The implemented algorithm uses iris information from both global and local iris data base. Each iris image is filtered with Log-Gabor filter and then a fixed length feature vector is obtained. The evaluation of the system achieved high confidence identity verification

based on iris texture using Log-Gabor transform; further efforts should be applied to improve iris localization stage.

Acknowledgment

This work was support by IPN- SIP20090041.

References

1. J. G. Daugman. "High confidence visual recognition of person by a test of statistical independence". *IEEE Trans. Pattern Analysis and Machine Intelligence*. Vol.25. pp. 1148–1161. Nov. 1993.
2. Daugman J. "New methods in iris recognitions". *IEEE Transactions on Systems, Man and Cybernetics –B* 37. pp. 1167–1175. Oct. 2007.
3. R. P. Wildes. "Iris recognition: an emerging biometric technology". *Proc. IEEE*. Vol.85. pp. 1348–1363. Sep. 1997.
4. L. Ma, T. Tan, Y. Wang, and D. Zhang. "Personal identification based on iris texture analysis". *IEEE Trans. Pattern Analysis and Machine Intelligence*. Vol.85. pp. 1519–1533. Sep. 1997.
5. LI identity solutions. Available from: <http://www.liid.com/pages/17>, 2009 (accessed March 2009).
6. LG. Available form: <http://www.lgiris.com/>, 2009 (accessed March 2009).
7. Sagem Morpho. Available from: <http://www.morpho.com/>, 2009 (accessed March 2009).
8. Li Yu, David Zhang, Kuanquan W. "The relative distance of key point based iris recognition". *Pattern Recognition*. Vol.40. pp. 423–430. 2007.
9. J.F.Canny. "Finding edges and lines in images". M.S. thesis. Mass. Inst. Technologies. 1983.
10. R.P.Wildes, J.C.Asmuth, G.L.Green. "A System for Automated Recognition". 0-8186-6410-X/94, IEEE. 1994.
11. P.V.C.Hough. "Method and means for recognizing complex patterns". U.S. Patent 3 069 654, 1962.
12. Sánchez Avila, C Sánchez Refillo. "Two Different Approaches for Iris Recognition using Gabor Filters and Multiscale Zero-Crossing Representación". *Pattern Recognition*. Vol.38.nº23. July 2004.
13. John Daugman, "Uncertainly relation for resolution in space, spatial frequency, and orientation optimized by two dimensional visual cortical filters". *J Opt. Soc. Amer. A*. Vol.2. pp.1160–1169. 1985.
14. D. Field. "Relations between the statics of natural images and the response proprieties of cortical cells". *Journal of the Optical Society of America*. 1987.
15. Chong S, Andrew T, David N. "High security Iris verification system based on random secret integration". *Computer Vision and Image Understanding*. Vol 102, Issue 2. May 2006. pp.169–177.
16. "CASIA" iris image database collected by institute of automation, Chinese academy of sciences. Available: www.sinobiometrics.com.
17. Tisee et all. "Person identification technique using human iris recognition", *Proc of Vision Inteface*, pp.294–299, 2002.